Pharmaceutical Research, Vol. 26, No. 5, May 2009 (© 2009)
DOI: 10.1007/s11095-009-9830-5

Research Paper

Noninvasive Monitoring of HPMA Copolymer–RGDfK Conjugates by Magnetic Resonance Imaging

Bahar Zarabi,[1,2] Mark P. Borgman,[1,2] Jiachen Zhuo,[3] Rao Gullapalli,[2,3] and Hamidreza Ghandehari[4,5,6]

Received October 30, 2008; accepted January 12, 2009; published online January 22, 2009

Purpose. To evaluate the tumor targeting potential of *N*-(2-hydroxypropyl)methacrylamide (HPMA) copolymer–gadolinium(Gd)–RGDfK conjugates by magnetic resonance (MR) T1-mapping.
Methods. HPMA copolymers with and without RGDfK were synthesized to incorporate side chains for Gd chelation. The conjugates were characterized by their side-chain contents and r_1 relaxivity. *In vitro* integrin-binding affinities of polymeric conjugates were assessed via competitive cell binding assays on HUVEC endothelial cells and MDA-MB-231 breast cancer cells. *In vivo* MR imaging was performed on MDA-MB-231 tumor-bearing SCID mice at different time points using non-targetable and targetable polymers. The specificity of $\alpha v\beta 3$ targeting was assessed by using non-paramagnetic targetable polymer to block $\alpha v\beta 3$ integrins followed by injection of paramagnetic targetable polymers after 2 h.
Results. The polymer conjugates showed relaxivities higher than Gd-DOTA. Endothelial cell binding studies showed that IC_{50} values for the copolymer with RGDfK binding to $\alpha v\beta 3$ integrin-positive HUVEC and MDA-MB-231 cells were similar to that of free peptide. Significantly lower T1 values were observed at the tumor site after 2 h using targetable conjugate ($p<0.012$). *In vivo* blocking study showed significantly higher T1 values ($p<0.045$) compared to targetable conjugate.
Conclusion. These results demonstrate the potential of this conjugate as an effective targetable MR contrast agent for tumor imaging and therapy monitoring.

KEY WORDS: contrast agents; HPMA copolymers; MRI; targeted delivery; tumor targeting.

INTRODUCTION

The ultimate goal of targeted imaging is to achieve a large contrast enhancement at the diseased site. The use of targetable radioligands has provided a means of generating tumor-specific contrast enhancement in nuclear scintigraphy (1). Due to lower sensitivity of conventional gadolinium enhanced magnetic resonance imaging (MRI), higher concentration of targeting moieties will be needed to specifically localize the contrast agent around the tumor and significantly reduce the local proton relaxation times (2,3). One strategy to solve this problem is to use polymers that are capable of carrying a large number of chelating agents and targeting moieties. This approach has been successfully applied in several *in vivo* MR imaging studies using monoclonal antibodies (4,5). However, targeting to tumors by antibodies remains a challenge because of relatively fewer antigen-binding sites on tumor cells and potential for immunogenicity.

The $\alpha_V\beta_3$ integrin is over expressed on both endothelial and tumor cells (6). This over expression correlates

[1] Department of Pharmaceutical Sciences, University of Maryland, Baltimore, Baltimore, Maryland, USA.
[2] Center for Nanomedicine and Cellular Delivery, University of Maryland, Baltimore, Baltimore, Maryland, USA.
[3] Department of Radiology, University of Maryland, Baltimore, Baltimore, Maryland, USA.
[4] Departments of Pharmaceutics & Pharmaceutical Chemistry and Bioengineering, University of Utah, 383 Colorow Road, Room 343, Salt Lake City, Utah 84108, USA.
[5] Center for Nanomedicine, Nano Institute of Utah, University of Utah, Salt Lake City, Utah, USA.
[6] To whom correspondence should be addressed. (e-mail: hamid.ghandehari@pharm.utah.edu)

ABBREVIATIONS: AIBN, Azobisisobutyronitrile; APMA, *N*-(3-Aminopropyl)methacrylamide hydrochloride; APMA-DOTA, *N*-methacryloylaminopropyl-2-(4-isothiourea-benzyl)-1,4,7,10-tetraazacyclododecane-1,4,7,10-tetraacetic acid; ATCC, American type culture collection; α, Flip angle; DMF, *N,N*-dimethylformamide; DMSO, Dimethyl sulfoxide; DOTA, 1,4,7,10-tetra-azacylcododecane-*N*,*N′*,*N″*, *N‴*-tetraacetic acid; EDTA, Ethylenediaminetetraacetic acid; FOV, Field of view; FPLC, Fast protein liquid chromatography; Gd, Gadolinium; $GdCl_3.6H_2O$, Gadolinium chloride; HPLC, High pressure liquid chromatography; HPMA, N-(2-hydroxypropyl)methacrylamide; HUVEC, Human umbilical vein endothelial cell; ICP-OES, Inductively coupled plasma optical emission spectroscopy; IDL, Interactive data language; kDa, Kilo dalton; MA-GG-ONp, *N*-methacryloylglycylglycyl-p-nitrophenyl ester; MA-GG-RGDfK, *N*-methacryloylglycylglycyl-RGDfK; MR, Magnetic resonance; MRI, Magnetic resonance imaging; M_w, Molecular weight; M_wCO, Molecular weight cut off; PBS, Phosphate buffered saline; RGD, Arg-Gly-Asp; RGD4C, Lys-Ala-Cys-Asp-Cys-Arg-Gly-Asp-Cys-Phe-Cys-Gly; RGDfK, Arg-Gly-Asp-D-Phe-Lys; r_1, Longitudinal relaxivity; ROI, Region of interest; S, Signal intensity; SCID, Severe combined immunodeficient; SEC, Size exclusion chromatography; T1, Longitudinal relaxation time; TE, Echo time; TEF, Trifluoroacetic acid; TR, Repetition time.

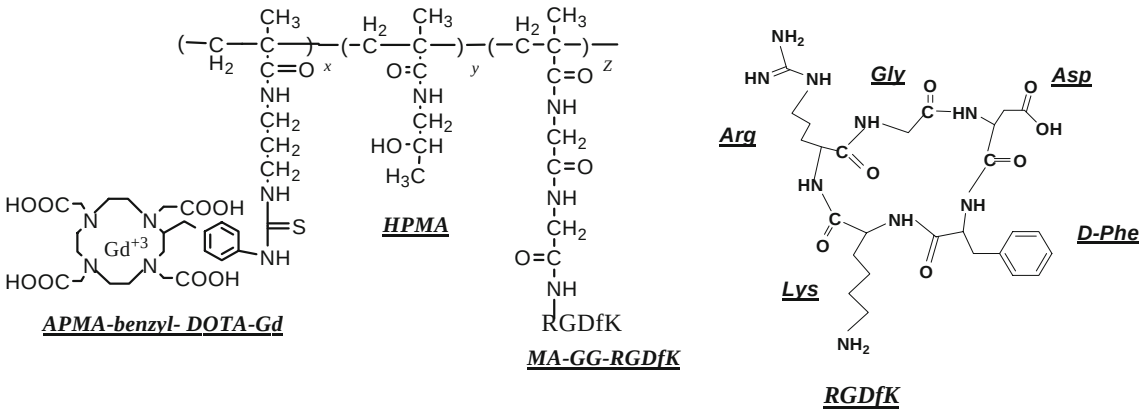

Fig. 1. Structure of HPMA copolymer–(Gd-DOTA)–RGDfK conjugates. (*HPMA N*-(2-hydroxypropyl)methacrylamide, *APMA-benzyl-DOTA* aminopropylmethacrylamide-benzyl-1,4,7,10 tetraazacyclododecane-1,4,7,10-tetraacetic acid, *Gd* gadolinium, *MA-GG-RGDfK N*-methacryloylglycylglycyl-RGDfK).

well with tumor progression and invasiveness (7–11). Studies in our laboratory with radiolabeled *N*-(2-hydroxypropyl)methacrylamide (HPMA) copolymers containing cyclized Arg-Gly-Asp (RGD) motifs in the side chains that target the $\alpha_V\beta_3$ integrins show enhanced tumor accumulation compared to non-targeted copolymers (12–14). Attachment of cyclic RGD4C in the side chains of HPMA copolymers resulted in a four to fivefold enhancement of accumulation in prostate tumors compared to the copolymers without the targeting peptide (12). Both monocyclic RGDfK and bicyclic RGD4C when attached to the copolymers showed similar accumulation patterns in Lewis lung carcinoma (15). Compared to peptides, copolymer–peptide conjugates showed lower accumulation in non-target background organs such as liver and spleen (13). The binding affinity of the conjugates and their biodistribution were controlled by varying the molecular weight, peptide content and charge of the conjugates (16). These conjugates show potential in targeted delivery of bioactive agents to solid tumors (14).

The molar relaxivity of MR contrast agents increases when attached to HPMA copolymers by reducing rotational correlation motion (17–21). HPMA copolymer-Gd chelates are nontoxic in a panel of cell lines (21). Conjugates of HPMA copolymer-Gd with doxorubicin exhibited 1.6 times higher relaxivity than the polymeric complex without Dox (21). These conjugates are stable under a range of pH. HPMA copolymers are in clinical trials for the treatment of several malignancies (22). Determining the fate of these systems by MRI allows monitoring the localization of the conjugates in solid tumors and can lead to the development of a new generation of MR contrast agents with HPMA copolymers.

In this study, we evaluated the targeting potential of HPMA copolymer–RGDfK–Gd conjugates (Fig. 1) using magnetic resonance (MR) T1-mapping of breast tumors in mice. T1-mapping is a quantitative MRI technique that allows measurement of the T1 values of water protons of different tissues. The synthesis, characterization, *in vitro* cell binding, and *in vivo* MR T1-mapping of HPMA copolymer–RGDfK–Gd conjugates are reported.

MATERIALS AND METHODS

Chemicals and Reagents

^{125}I-echistatin (2000 Ci/mmol) was purchased from GE Healthcare (Piscataway, NJ). RGDfK (MW 604.5) was obtained from AnaSpec Inc. (San Jose, CA). *N*, *N*′-azobisisobutyronitrile (AIBN) and gadolinium (III) chloride hexahydrate (GdCl3.6H2O) were obtained from Aldrich (Milwaukee, WI, USA). *N*-(3-aminopropylmethacrylamide (APMA) was obtained from Polysciences, Inc. (Warrington, PA, USA). p-isothiocyanatobenzyl-1, 4, 7, 10 tetraazacyclododecane-1, 4, 7, 10 tetraacetic acid (p-SCN-Bz-DOTA) was obtained from Macrocyclics (Dallas, TX, USA). *N*, *N*, *N*′, *N*′-ethylenediaminetetraacetic acid (EDTA) disodium salt dihydrate was obtained from USB Corporation (Cleveland. OH, USA). All other chemicals were purchased from Sigma (St. Louis, MO, USA) and were of reagent grade.

Cell Lines

Human breast cancer cell line MDA-MB-231 (ATCC, Manassas, VA) was cultured in RPMI-1640 (ATCC, Manassas, VA) medium supplemented with 10% Fetal Bovine Serum (Quality Biological) and 1% Penicillin-Streptomycin (Mediatech, Manassas, VA) in a 37°C incubator. All cells were grown to 80–90% confluency before trypsinization and formulation in HBSS (Mediatech, Manassas, VA) for implantation into mice. Human Umbilical Vein Endothelial Cells (HUVECs) were cultured in endothelial cell growth media-2 (EGM-2: Lonza, Walkersville, MD) in a humidified atmosphere of 5% CO2 (*v*/*v*) at 37°C. For binding studies, confluent cells (MDA-MB-231& HUVECs) were harvested with 0.05% trypsin/0.02% EDTA in PBS.

Synthesis and Characterization of Comonomers

N-(2-hydroxypropyl)methacrylamide (HPMA) (23), *N*-methacryloylglycylglycyl-p-nitrophenyl ester (MA-GG-ONp) (24), and gadolinium(Gd) chelating comonomer aminopropylmethacrylamide-benzyl-1,4,7,10 tetraazacyclododecane-

1,4,7,10 tetraacetic acid (APMA-benzyl-DOTA) (20) were synthesized and characterized by previously described methods. *N*-methacryloylglycylglycyl-RGDfK (MA-GG-RGDfK, MW 786.9) was synthesized via p-nitrophenyl ester aminolysis of MA-GG-ONp in dry DMF in the presence of pyridine for 48 h. Resulting product was purified using preparatory HPLC (Varian Prostar, Palo Alto, CA) with a Microsorb 100 C-18 reversed phase column (250×10 mm) using a gradient mixture of water with 0.1% trifluoroacetic acid (TFA) and acetonitrile with 0.1% TFA at 2 ml/min. The product was monitored by UV spectrophotometry (λ=220 nm), and elution peaks pooled and lyophilized.

Synthesis and Characterization of Copolymers

HPMA copolymer precursors were synthesized by free radical precipitation copolymerization. First the polymers were synthesized using monomers of HPMA, APMA-benzyl-DOTA, and MA-GG-RGDfK in predetermined molar compositions (Table I). All polymerizations were carried out in 100% of DMSO using AIBN as the initiator and 3-mercaptopropionic acid (0.015 mol%) as a chain transfer agent to control the molecular weight of the copolymers. The ratio of monomers: initiator: solvent in the feed were kept constant at 12.5: 0.6: 86.9 (wt.%), respectively. The comonomer mixtures were sealed in an ampoule under nitrogen and stirred at 50°C for 24 h. DMSO was evaporated and the copolymers were dissolved in deionized water and dialyzed (MWCO=3500) against deionized water for 48 h followed by lyophilization. The DOTA content was assessed using UV spectrophotometry (λ=274 nm). The peptide (RGDfK) content of the side chains was determined by amino acid analysis (Commonwealth Biotechnologies, Richmond, VA). In the second step, polymeric conjugates were chelated to Gd. Gadolinium (III) chloride hexahydrate (GdCl3.6H2O) (1.5:1 molar equivalents relative to the DOTA content of the feed) were dissolved in de-ionized water (for nontargetable polymer) or acetate buffer (for targetable polymer). The pH of the solution was maintained at 5–5.5 overnight. Excess of Gd was removed using EDTA disodium salt dehydrate (EDTA: Gd, 1:1). Afterwards, the solutions were purified on a PD10 size exclusion column (GE Healthcare, NJ, USA). The polymer conjugates were dialyzed for 48 h and lyophilized. Copolymer Gd contents were determined using Inductively Coupled Plasma Optical Emission Spectroscopy (ICP-OES) (Galbraith, Knoxville, TN). The weight average molecular weight and molecular weight distribution of the polymeric conjugates were estimated by size exclusion chromatography (SEC) on a Superose 12 HR 10/30 column (GE Healthcare, Piscataway, NJ) using a Fast Protein Liquid Chromatography (FPLC) system (GE Healthcare) and HPMA homopolymer fractions of known molecular weight as calibration standards.

Relaxivity Measurements

Nontargetable HPMA copolymer–(Gd-DOTA) and targetable HPMA copolymer–(Gd-DOTA)–RGDfK conjugates were prepared in four different concentrations (from 0.1 to 0.015 mM). T1 of these solutions and deionized water were determined on a 1.5 T MR system (Eclipse, Philips Medical System, Cleveland, OH). T1 was measured by an inversion recovery fast spin echo imaging sequence using inversion times of 50, 100, 200, 400, 700, 1400, 2000, and 2800 ms, an echo time (TE) of 12 ms, and an echo train length of 8 at a repeat time (TR) of 6000 ms. All images were obtained from a single axial slice with a 20×15 cm field of view (FOV), 3 mm slice thickness, 256×192 matrix and one excitation. T1 for each solution and deionized water were calculated using MATLAB (The Mathworks, Inc., Natick, MA). The relaxivity (r1) value was calculated from the slope of the plot of (1/T1, solution −1/T1, water) *versus* equivalent concentration of Gd, where T1, solution is the T1 of each dilution of the contrast agent and T1, water is the T1 of water without contrast agent.

Binding Assay

In vitro integrin binding affinities of free RGDfK peptide and HPMA copolymer–RGDfK conjugates were assessed via a competitive cell binding assay using ^{125}I-echistatin as $\alpha_v\beta_3$ integrin-specific radioligand (25,26) on HUVECs and MDA-MB-231 as previously described (16). Briefly, cells were harvested, washed with PBS, resuspended in binding buffer containing 20 mmol/L Tris, 150 mmol/L NaCl, 2 mmol/L $CaCl_2$, 1 mmol/L $MgCl_2$, 1 mmol/L $MnCl_2$, 0.1% bovine serum albumin, pH 7.4, and seeded at 50,000 cells per well in 96-well Multiscreen HV filter plates (0.45 μm; Millipore). Cells were co-incubated with ^{125}I-echistatin (0.05 nM) and increasing peptide equivalent concentrations of polymers or free RGDfK (0–100 μM) for 2 h with gentle agitation at 4°C. The final volume was adjusted to 200 μL in binding buffer. In

Table I. Physicochemical Characteristics of HPMA Copolymer–Contrast Agent Conjugates

	Feed comonomer composition (mol%)			Side chain contents (mmol/g polymer)		M_w[b] (g/mol)	n[c]	Relaxivity (s^{-1} mM^{-1}Gd)
Samples[a]	HPMA	DOTA	RGDfK	RGDfK content	Gd content			
P-Gd	90	10	–	–	0.41	45,000	1.5	19.8
P-RGDfK-Gd	70	10	20	0.428	0.14	43,000	1.5	20.6

[a] For structures of polymer-contrast agent conjugates see Fig. 1
[b] Weight average molecular weight of polymer precursor
[c] Polydispersity index

the next step, the plates were filtered using a Multiscreen vacuum manifold (Millipore, Billerica, MA) and washed twice with cold binding buffer. Filters were removed and counted by gamma scintillation (Perkin Elmer Wizard, 1470 Automatic Gamma Counter). Nonspecific binding was measured in the presence of 200-fold molar excess of cold echistatin. The IC_{50} values were determined by nonlinear regression analysis using GraphPad Prism (GraphPad Software, Inc.). Each data point represents the average of values of triplicate wells.

Animal Tumor Model

The animal studies were carried out at Johns Hopkins University School of Medicine Molecular Imaging Center. Female SCID mice (4–6 weeks old) were purchased from the National Cancer Institute (Frederick, MD). The mice were cared for according to the guidelines of the Institutional Animal Care and Use Committee of Johns Hopkins University and all studies were carried out in full compliance with institutional guidelines related to the conduct of animal experiments. 1×10^6 to 5×10^6 MDA-MB-231 cells formulated in 100 μl HBSS were implanted into the right mammary fat pad of female SCID mice. MRI experiments were carried out when the tumor size reached 0.3–0.5 cc.

MR Imaging and T1-Mapping

Each anesthetized mouse was immobilized in the probe and maintained under gas anesthesia (1% isoflurane mixed with air at 1 l/min). The polymer conjugates were injected intravenously via the lateral tail vein at a dose of 0.03 mmol-Gd/kg. Each contrast agent was studied in a group of four mice. Blocking studies were performed in a group of three mice. In these studies first mice were injected with targetable conjugate without Gd and after 2 h with Gd-chelated targetable conjugate. MR studies were performed on a 9.4 tesla Bruker Biospec spectrometer with a 35 mm volume coil before and at various time points after injection. Quantitative T1 MR images were obtained by a saturation-recovery multislice spin-echo pulse sequence using the following equation:

$S=[S_0\ (1\text{-}f)\ \sin(\alpha)]/[1\text{-}f\ \cos(\alpha)]$, where $f=\exp(\text{-TR/T1})$, S is signal intensity, S_0 is a constant describing the imager gain and proton attenuation and α is the flip angle. Saturation-recovery T1 axial images of the tumor section (slice thickness of 2 mm, 3 or 4 slices for each tumor) were acquired with six relaxation delays of 250 ms, 500 ms, 1 s, 2 s, 4 s, and 8 s with an in-plane spatial resolution of 0.250 mm (128×64 matrix zero filled to 128×128, field of view=32 mm, number of scans=8). Quantitative T1 relaxation maps were reconstructed from datasets for six different relaxation times using the IDL (Interactive Data Language, Boulder, CO). The color values were assigned using ImageJ software (National Institute of Health, MD). Multislice T1 weighted coronal images of the mice body were also acquired with a relaxation delay of 1 sec with a final matrix size of 256×128 (field of view 48×28×28 mm).

Regions of interest (ROI) were defined along the tumor rim from which T1-values were obtained before and after injection of contrast agents.

Statistical Analysis

Statistical analyses were performed using two-tailed unpaired student *t*-test (GraphPad Prism, GraphPad software, San Diego, CA). Difference was considered significant when $p<0.05$.

RESULTS

Physicochemical Characteristics of the Conjugates

The molecular weight, molecular weight distribution and side chain content of the copolymers with or without peptide are reported in Table I. The incorporation of MA-GG-RGDfK was 70% of the feed content. The copolymers contained on average approximately 17 RGDfK per polymer backbone. The incorporation of APMA-DOTA in targetable and nontargetable polymers was 70% and 94% respectively of the feed content. Gd chelation to the DOTA side chains of the conjugates resulted in Gd incorporation efficiency of 70% and 87% of the DOTA molecules per polymer backbone with and without RGDfK respectively. The number of Gd per polymer chain for targetable and nontargetable polymers were approximately 6 and 18 respectively. Both conjugates showed higher relaxivities (r_1) than the commercially available Gd-DOTA contrast agent (Dotarem®) (27).

In Vitro Binding of the Conjugates

The binding affinity of HPMA copolymer–RGDfK conjugate in the presence of radiolabeled echistatin was evaluated using integrin $\alpha_v\beta_3$-positive HUVECs and MDA-MB-231 cell lines. Both cyclic RGDfK peptide and HPMA copolymer–RGDfK conjugate inhibited the binding of ^{125}I-echistatin to cell lines. The percent bound ^{125}I-echistatin (Fig. 2) was decreased with an increase in copolymer concentration. IC_{50} values (nM peptide) for polymeric conjugate and free peptide were 1503±1.62 and 1311±1.6 for HUVECs and 4764±1.85 and 3984±1.14 for MDA-MB-231 respectively. The results show that peptides attached to polymeric backbones remain effective for targeting $\alpha_v\beta_3$ integrins.

MRI Enhancement of Polymeric Conjugates

The time dependent biodistribution of polymer–peptide–gadolinium conjugates at the tumor site was evaluated using MR T1 mapping. Fig. 3 shows the coronal T1-weighted MR images of tumor bearing mice before and at 10 min, 30 min, 1, 2, 6, 24 h after injection of polymeric contrast agents. Both targetable and non-targetable conjugates resulted in signal enhancement in kidney up to 24 h. Fig. 4A and B show the axial color coded T1 maps of tumor bearing mice pre- and at 10 min, 30 min, 1, 2, 6, 24 h post-injection of contrast agents. The calibration bar indicates T1 values related to each color. White color (top) and blue color (bottom) show the highest and the lowest T1 values respectively. The mean T1 values for targetable and nontargetable contrast agent are (pre: 2435±236.8 ms and 2 h: 1950±189.8 ms) and (pre: 2423±175.5 ms and 2 h: 2127±144 ms) respectively. At this time point the targeted conjugate showed significant decrease in T1 values

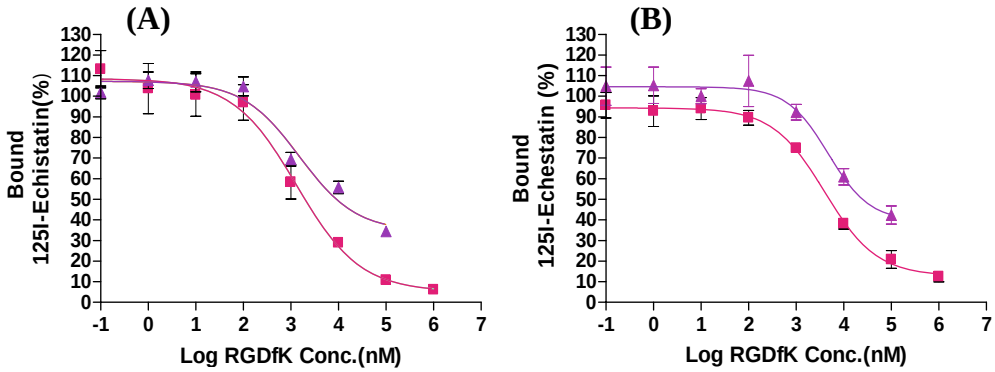

Fig. 2. Competitive binding of HPMA copolymer–(DOTA-Gd)–RGDfK conjugates (*filled triangle*) and free peptide (*filled square*) to: **A** HUVECs and **B** MDA-MB-231 cells. Results are expressed as means of triplicate ± SD.

at the tumor site compared to non-targeted conjugate ($p < 0.012$) (Fig. 5). There was no significant difference between targetable and non-targetable contrast agents at other time points. Fig. 4C shows the involvement of $\alpha_v\beta_3$ integrins in changes in T1 values at the tumor site. Blocking the integrins with targetable conjugate (without Gd) resulted in significant increase in T1 values compared to Gd chelated targetable conjugate ($p < 0.045$).

DISCUSSION

Recent progress in molecular targeting and cancer therapeutics has added a new dimension to the imaging sciences. MRI with macromolecular contrast agents, which are capable of carrying large number of gadolinium and targeting moieties, may offer some assistance in more specific and probably more accurate tumor characterization. In this study HPMA copolymer–RGDfK conjugates were labeled with gadolinium to explore the MR imaging of these systems in solid tumors. This strategy has several advantages that are desirable for targeted delivery and imaging applications. First, the conjugates are known to localize in solid tumors. Second, the copolymer architecture can be manipulated with relative ease to allow control over binding, localization and excretion. Third, the multivalency of the targeting moieties and contrast agents in the polymeric conjugates would result in better targeting properties and imaging effect (15).

The effective dose of macromolecular contrast agents for tumor imaging is between 0.03–0.1 mmol-Gd/kg (28). In this study a lower dose (0.03 mmolGd/Kg) was used in order to avoid a strong background signal in combination with a higher magnetic field strength of 9.4 Tesla for improved signal to noise ratio (29). High field MR systems can expand the ability to fully characterize neoplastic lesions as well as monitoring the effects of therapy.

The average molecular size of the conjugates (~43–45 kDa) was around the glomerular filtration threshold (45 kDa) for HPMA copolymers (30). This is the optimal size for effective clearance of the polymer from the body over time. Biodistribution studies of HPMA-based contrast agents showed that HPMA copolymer–Gd conjugates with high molecular weight had a prolonged blood circulation time and high passive tumor targeting efficiency (19). Non-biodegradable HPMA copolymer–Gd conjugates with molecular weights higher than the threshold of renal filtration demonstrated higher efficiency for tumor drug delivery than biodegradable poly(L-glutamic acid) conjugates (19). We have previously observed that HPMA copolymer–RGDfK conjugates with side chains terminated in negatively charged chelating agents preferentially accumulate in the kidney (16). For the present polymers the kinetics of kidney accumulation

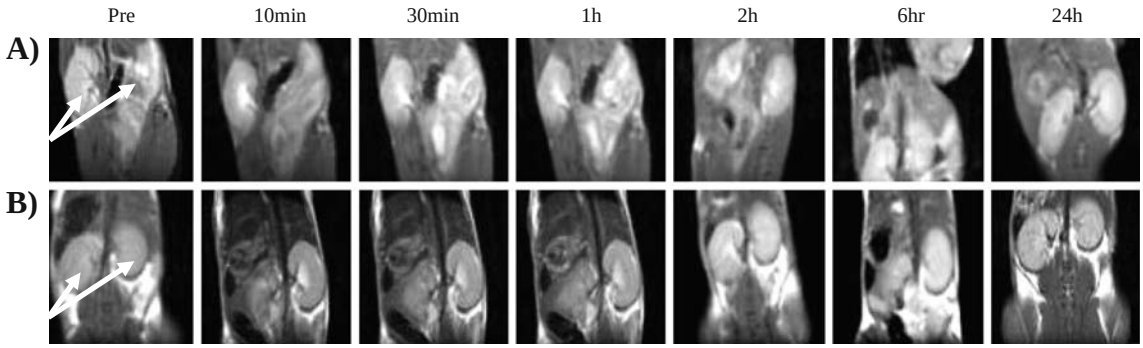

Fig. 3. T1-weighted contrast enhanced coronal MR images of SCID mice bearing human breast cancer cell line (MDA-MB-231) xenografts before and after injection of HPMA copolymer–(DOTA-Gd) (**A**) and HPMA copolymer–(DOTA-Gd)–RGDfK (**B**) conjugates. The *arrow* shows the kidney.

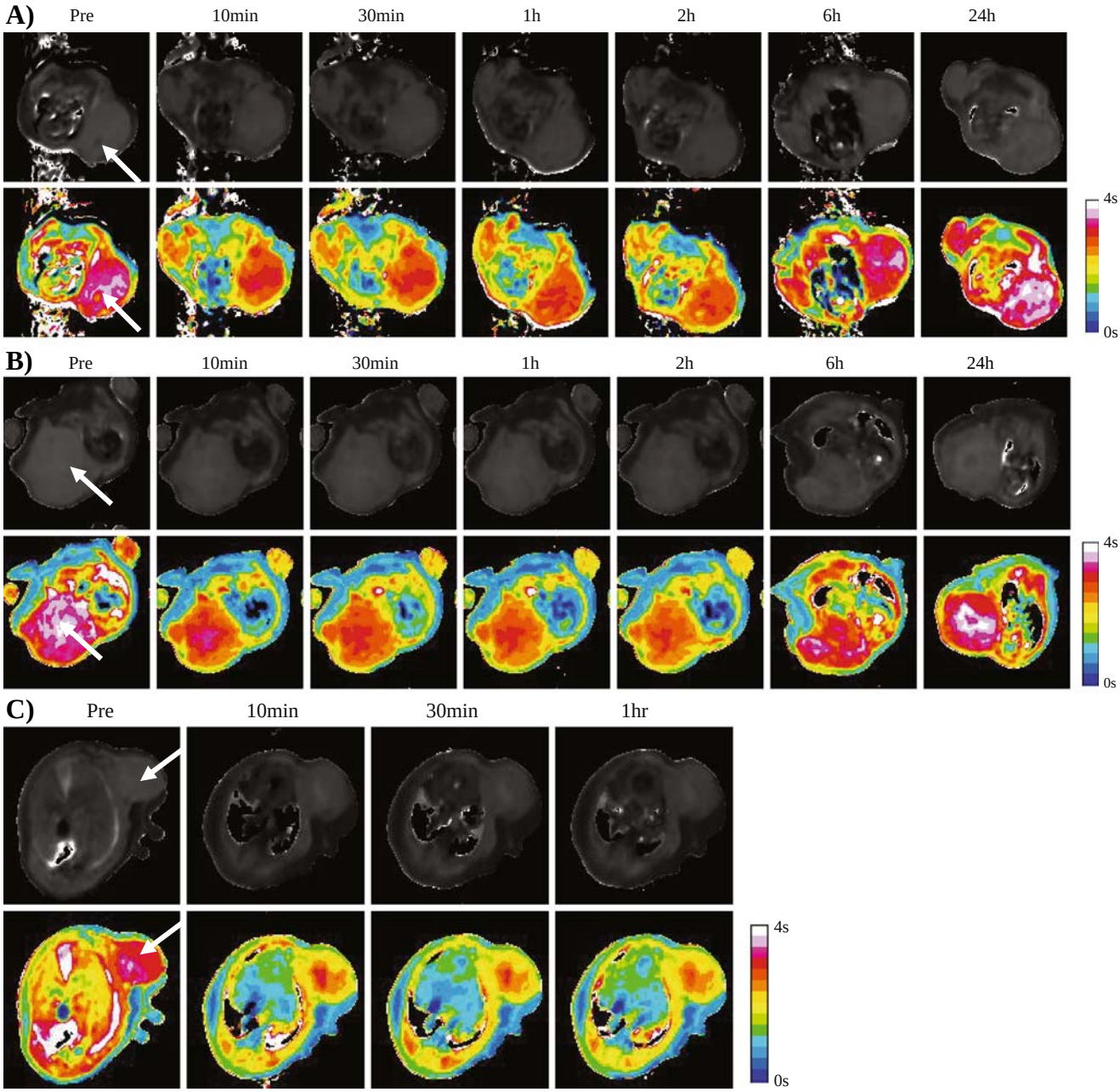

Fig. 4. T1-maps of contrast enhanced axial MR images of SCID mice bearing human breast cancer cell line (MDA-MB-231) xenografts before and after injection of HPMA copolymer–(DOTA-Gd) conjugate (**A**), HPMA copolymer–(DOTA-Gd)–RGDfK conjugate (**B**), and HPMA copolymer–(DOTA)–RGDfK conjugate followed by injection of HPMA copolymer–(DOTA-Gd)–RGDfK conjugate after 2 h (**C**). The *arrow* shows the tumor. The color scale shown is reflective of T1-values. The arrival of the contrast reduces the T1-value of the tumor as seen by the color differences and begins to normalize back to its original value after about 6 h.

and potential Gd-induced nephrotoxicity of the conjugates need to be investigated. The relaxivity of HPMA copolymer contrast agent conjugates were improved over commercially available contrast agent Gd-DOTA (Table I). This has been observed for several macromolecular contrast agents including HPMA copolymer based contrast agents (31–34).

Relatively high concentration of peptide (~17 peptides) was incorporated in the RGDfK containing HPMA-(Gd-DOTA) conjugate to achieve better tumor targeting. The *in vitro* binding studies demonstrated that RGDfK containing copolymer remained effective for targeting $\alpha_v\beta_3$ integrins. The binding affinity of polymer-RGDfK conjugate is lower than free RGDfK on both HUVECs and MDA-MB-231 human breast cancer cell line probably due to steric hindrance of the polymers. This finding is in agreement with previous studies (16). The binding of HPMA copolymer–RGDfK conjugates to MDA-MB-231 cell lines as well as HUVECs demonstrates that such conjugates may be used for the delivery of both anti-angiogenic and antitumor drugs.

Previously, the effectiveness of RGD containing HPMA copolymers for targeting $\alpha_v\beta_3$ integrins was evaluated by

scintigraphy (12,13,15). One of the advantages of MRI compared to scintigraphy is its high spatial resolution. Correlation of drug localization in the target tissue with the local pathologic features, such as changes in tumor type, size and stage, may help optimize the structure of the drug delivery systems for personalized medicine. One of the limitations of conventional MRI with the currently available contrast agents is its relatively low sensitivity in targeting and staging tumors. MR T1-mapping technique provides a quantitative means (35) to assess changes in the relaxation time (T1 values) after administration of magnetic resonance contrast agents. The Gd concentration is proportional to the longitudinal relaxation rate. In this study, T1 values at tumor periphery decreased significantly during the initial period after injection for all conjugates (Fig. 4). However, after 2 h (Fig. 5), a significant difference ($p<0.012$) between the mean T1 values at the tumor site using HPMA copolymer–(Gd-DOTA) was found with and without the peptide. After 6 h, increase in mean T1 values was observed within the tumor suggesting washout of the contrast from the tumor. This observation could be due to the presence of negative charges in the side chains and therefore high renal excretion of the polymers (16). At 24 h, post-injection, T1 values almost returned to the pre-injection level at the tumor site. Kidney images indicate rapid initial renal accumulation of the conjugates (Fig. 3). Sustained kidney activity over time suggests that these conjugates are entrapped and also eliminated through the kidney. Non-targetable HPMA copolymer–Gd conjugates (19) and HPMA copolymer–RGDfK conjugates with molecular weight under the glomerular filtration threshold (45 kDa) (15) are known to accumulate and be excreted via the kidney over a period of few days.

The effectiveness of RGD containing HPMA copolymer–(Gd-DOTA) conjugate for targeting $\alpha_v\beta_3$ integrins was also evaluated *in vivo* by a blocking study using MR T1-mapping. The targetable polymer without Gd probably occupied the large number of $\alpha_v\beta_3$ integrins, therefore subsequent administration of targetable polymer with Gd resulted in higher T1 values (Fig. 5). There is significant difference at all time points between the targetable polymer and T1 values observed in the blocking study ($p<0.045$).

Profiling each patient for stage of the disease, presence of cancer targets before initiation of therapy and the ability to follow the fate of drug delivery systems such as HPMA copolymer–drug conjugates in individual patients can improve efficacy of therapy while reducing side effects. The present study is a step towards that goal by developing a MR contrast agent targetable to $\alpha_v\beta_3$ integrins. To make this approach clinically viable the future immediate steps are to: (1) Optimize Gd content in the targetable polymer for better enhancement of images; (2) Use higher molecular weight conjugates for higher accumulation and better enhancement at the tumor site, and (3) Use higher concentrations of contrast agents to further improve the *In vivo* contrast enhancement. Development of imaging technologies for targeted drug delivery systems can have a major impact in cancer therapy, where images are used to define target volumes for therapy, dose optimization, guiding surgical intervention, monitoring response to therapy and establishing individualized patient treatment strategies (36).

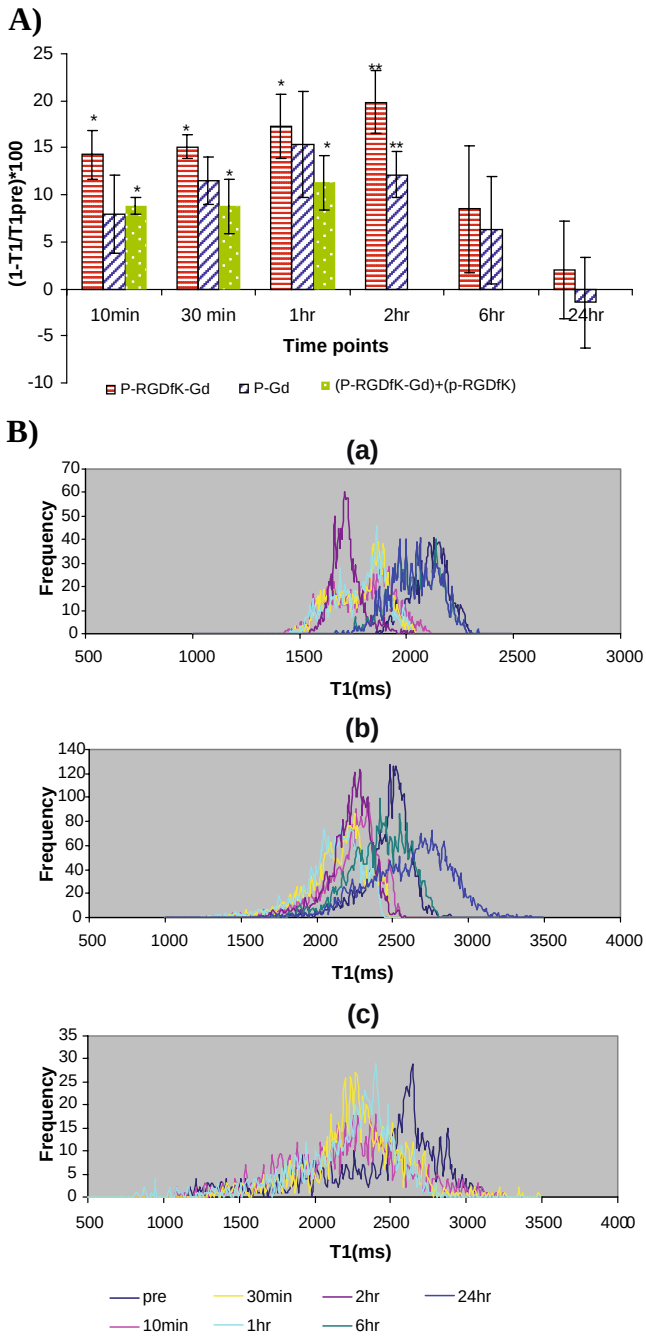

Fig. 5. *Top panel* **A** Comparison of mean T1 values at tumor site at different time points. Data is expressed as mean±SD. Number of mice/group is four for P-RGDfK-Gd and P-Gd groups and three for P-RGDfK-Gd+P-RGDfK group. *Bottom panel* **B** T1 histograms of MDA-MB-231 tumors at different time points after injection of (*a*) HPMA copolymer–(DOTA-Gd)–RGDfK, (*b*) HPMA copolymer–(DOTA-Gd), and (*c*) HPMA copolymer–(DOTA)–RGDfK conjugate followed by injection of HPMA copolymer–(DOTA-Gd)–RGDfK conjugate after 2 h.

CONCLUSION

In conclusion, the HPMA copolymer–(Gd-DOTA)–cyclic RGD conjugate was effective for noninvasive $\alpha_v\beta_3$ integrin imaging of MDA-MB-231 breast tumors using

quantitative MR T1-mapping. These results show the potential of these targetable conjugates as effective MR contrast agents for tumor imaging and evaluating the fate of targetable HPMA copolymer drug delivery systems.

ACKNOWLEDGMENT

This study received financial support from the Department of Defense Breast Cancer Research Program predoctoral fellowship to Bahar Zarabi (W81XWH0410341) and a grant from the National Institute of Biomedical Imaging and Bioengineering (R01-EB007171). The authors acknowledge Mrudulla Pullambhatla and Wenlian Zhu at Johns Hopkins University School of Medicine Molecular Imaging Center for their assistance with *in vivo* MR imaging and facilitated by a grant from the National Cancer Institute (U24 CA92871).

REFERENCES

1. S. Erdogan, A. Roby, and V. P. Torchilin. Enhanced tumor visualization by gamma-scintigraphy with ^{111}In-labeled polychelating-polymer-containing immunoliposomes. *Mol. Pharm.* **3**:525–530 (2006). doi:10.1021/mp060055t.
2. W. T. Anderson-Berg, M. Strand, T. E. Lempert, A. E. Rosenbaum, and P. M. Joseph. Nuclear magnetic resonance and gamma camera tumor imaging using gadolinium-labeled monoclonal antibodies. *J. Nucl. Med.* **27**:829–833 (1986).
3. J. B. Mandeville, B. G. Jenkins, Y. C. Chen, J. K. Choi, Y. R. Kim, D. Belen, C. Liu, B. E. Kosofsky, and J. J. Marota. Exogenous contrast agent improves sensitivity of gradient-echo functional magnetic resonance imaging at 9.4 T. *Magn. Reson. Med.* **52**:1272–1281 (2004). doi:10.1002/mrm.20278.
4. G. Niu, W. Cai, and X. Chen. Molecular imaging of human epidermal growth factor receptor 2 (HER-2) expression. *Front Biosci.* **13**:790–805 (2008). doi:10.2741/2720.
5. H. Kim, D. E. Morgan, H. Zeng, W. E. Grizzle, J. M. Warram, C. R. Stockard, D. Wang, and K. R. Zinn. Breast tumor xenografts: diffusion-weighted MR imaging to assess early therapy with novel apoptosis-inducing anti-DR5 antibody. *Radiology*. **248**:844–851 (2008). doi:10.1148/radiol.2483071740.
6. W. A. Weber, R. Haubner, E. Vabuliene, B. Kuhnast, H. J. Wester, and M. Schwaiger. Tumor angiogenesis targeting using imaging agents. *Q. J. Nucl. Med.* **45**:179–182 (2001).
7. P. C. Brooks, R. A. Clark, and D. A. Cheresh. Requirement of vascular integrin alpha v beta 3 for angiogenesis. *Science*. **264**:569–571 (1994). doi:10.1126/science.7512751.
8. L. Bello, M. Francolini, P. Marthyn, J. Zhang, R. S. Carroll, D. C. Nikas, J. F. Strasser, R. Villani, D. A. Cheresh, and P. M. Black. Alpha(v)beta3 and alpha(v)beta5 integrin expression in glioma periphery. *Neurosurgery*. **49**:380–389 (2001)discussion 390.
9. D. Meitar, S. E. Crawford, A. W. Rademaker, and S. L. Cohn. Tumor angiogenesis correlates with metastatic disease, N-myc amplification, and poor outcome in human neuroblastoma. *J. Clin. Oncol.* **14**:405–414 (1996).
10. G. Gasparini, P. C. Brooks, E. Biganzoli, P. B. Vermeulen, E. Bonoldi, L. Y. Dirix, G. Ranieri, R. Miceli, and D. A. Cheresh. Vascular integrin alpha(v)beta3: a new prognostic indicator in breast cancer. *Clin. Cancer Res.* **4**:2625–2634 (1998).
11. S. Sengupta, N. Chattopadhyay, A. Mitra, S. Ray, S. Dasgupta, and A. Chatterjee. Role of alphavbeta3 integrin receptors in breast tumor. *J. Exp. Clin. Cancer Res.* **20**:585–590 (2001).
12. A. Mitra, J. Mulholland, A. Nan, E. McNeill, H. Ghandehari, and B. R. Line. Targeting tumor angiogenic vasculature using polymer-RGD conjugates. *J. Control. Release*. **102**:191–201 (2005). doi:10.1016/j.jconrel.2004.09.023.
13. B. R. Line, A. Mitra, A. Nan, and H. Ghandehari. Targeting tumor angiogenesis: comparison of peptide and polymer-peptide conjugates. *J. Nucl. Med.* **46**:1552–1560 (2005).
14. A. Mitra, A. Nan, J. C. Papadimitriou, H. Ghandehari, and B. R. Line. Polymer-peptide conjugates for angiogenesis targeted tumor radiotherapy. *Nucl. Med. Biol.* **33**:43–52 (2006). doi:10.1016/j.nucmedbio.2005.09.005.
15. A. Mitra, T. Coleman, M. Borgman, A. Nan, H. Ghandehari, and B. R. Line. Polymeric conjugates of mono- and bi-cyclic alphaVbeta3 binding peptides for tumor targeting. *J. Control. Release*. **114**:175–183 (2006). doi:10.1016/j.jconrel.2006.06.014.
16. M. P. Borgman, T. Coleman, R. B. Kolhatkar, S. Geyser-Stoops, B. R. Line, and H. Ghandehari. Tumor-targeted HPMA copolymer-(RGDfK)-(CHX-A"-DTPA) conjugates show increased kidney accumulation. *J. Control. Release*. **132**:193–199 (2008). doi:10.1016/j.jconrel.2008.07.014.
17. Y. Huang, A. Nan, G. M. Rosen, C. A. Winalski, E. Schneider, P. Tsai, and H. Ghandehari. N-(2-Hydroxypropyl)Methacrylamide (HPMA) copolymer-linked nitroxide: potential magnetic resonance contrast agent. *Macromol. Biosci*. **3**:647–652 (2003). doi:10.1002/mabi.200350031.
18. D. Wang, S. C. Miller, M. Sima, D. Parker, H. Buswell, K. C. Goodrich, P. Kopeckova, and J. Kopecek. The arthrotropism of macromolecules in adjuvant-induced arthritis rat model: a preliminary study. *Pharm. Res*. **21**:1741–1749 (2004). doi:10.1023/B:PHAM.0000045232.18134.e9.
19. Y. Wang, F. Ye, E. K. Jeong, Y. Sun, D. L. Parker, and Z. R. Lu. Noninvasive visualization of pharmacokinetics, biodistribution and tumor targeting of poly[N-(2-hydroxypropyl)methacrylamide] in mice using contrast enhanced MRI. *Pharm. Res.* **24**:1208–1216 (2007). doi:10.1007/s11095-007-9252-1.
20. B. Zarabi, A. Nan, J. Zhuo, R. Gullapalli, and H. Ghandehari. Macrophage targeted N-(2-hydroxypropyl)methacrylamide conjugates for magnetic resonance imaging. *Mol. Pharm.* **3**:550–557 (2006). doi:10.1021/mp060072i.
21. B. Zarabi, A. Nan, J. Zhuo, R. Gullapalli, and H. Ghandehari. HPMA Copolymer-doxorubicin-gadolinium conjugates: synthesis, characterization, and *in vitro* evaluation. *Macromol. Biosci.* **8**:741–748 (2008). doi:10.1002/mabi.200700290.
22. J. Kopecek, P. Kopeckova, T. Minko, and Z. Lu. HPMA copolymer-anticancer drug conjugates: design, activity, and mechanism of action. *Eur. J. Pharm. Biopharm.* **50**:61–81 (2000). doi:10.1016/S0939-6411(00)00075-8.
23. J. Strohalm, and J. Kopecek. Poly N-(2-hydroxypropyl) methacrylamide: 4. Heterogenous polymerization. *Angew. Makromol. Chem.* **70**:109–118 (1978). doi:10.1002/apmc.1978.050700110.
24. P. Rejmanova, J. Labsky, and J. Kopecek. Aminolyses of monomeric and polymeric p-nitrophenyl esters of methacryloylated amino acids. *Makromol. Chem.* **178**:2159–2168 (1977). doi:10.1002/macp.1977.021780803.
25. Y. Wu, X. Zhang, Z. Xiong, Z. Cheng, D. R. Fisher, S. Liu, S. S. Gambhir, and X. Chen. microPET imaging of glioma integrin {alpha}v{beta}3 expression using (64)Cu-labeled tetrameric RGD peptide. *J. Nucl. Med.* **46**:1707–1718 (2005).
26. C. C. Kumar, H. Nie, C. P. Rogers, M. Malkowski, E. Maxwell, J. J. Catino, and L. Armstrong. Biochemical characterization of the binding of echistatin to integrin alphavbeta3 receptor. *J. Pharmacol. Exp. Ther.* **283**:843–853 (1997).
27. J. C. Bousquet, S. Saini, D. D. Stark, P. F. Hahn, M. Nigam, J. Wittenberg, and J. T. Ferrucci Jr. Gd-DOTA: characterization of a new paramagnetic complex. *Radiology*. **166**:693–698 (1988).
28. T. Ke, E. K. Jeong, X. Wang, Y. Feng, D. L. Parker, and Z. R. Lu. RGD targeted poly(L-glutamic acid)-cystamine-(Gd-DO3A) conjugate for detecting angiogenesis biomarker alpha(v) beta3 integrin with MRT, mapping. *Int. J. Nanomedicine*. **2**:191–199 (2007).
29. J. E. Schneider, T. Lanz, H. Barnes, D. Medway, L. A. Stork, C. A. Lygate, S. Smart, M. A. Griswold, and S. Neubauer. Ultra-fast and accurate assessment of cardiac function in rats using accelerated MRI at 9.4 Tesla. *Magn. Reson. Med.* **59**:636–641 (2008). doi:10.1002/mrm.21491.
30. L. W. Seymour, R. Duncan, J. Strohalm, and J. Kopecek. Effect of molecular weight (M_w) of N-(2-hydroxypropyl)methacrylamide copolymers on body distribution and rate of excretion after subcutaneous, intraperitoneal, and intravenous administration to rats. *J. Biomed. Mater. Res.* **21**:1341–1358 (1987). doi:10.1002/jbm.820211106.
31. P. Caravan, M. T. Greenfield, X. Li, and A. D. Sherry. The Gd(3+) complex of a fatty acid analogue of DOTP binds to multiple

albumin sites with variable water relaxivities. *Inorg. Chem.* **40**:6580–6587 (2001). doi:10.1021/ic0102900.

32. P. Caravan, J. J. Ellison, T. J. McMurry, and R. B. Lauffer. Gadolinium(III) chelates as MRI contrast agents: structure, dynamics, and applications. *Chem. Rev.* **99**:2293–2352 (1999). doi:10.1021/cr980440x.
33. F. Kiessling, M. Heilmann, T. Lammers, K. Ulbrich, V. Subr, P. Peschke, B. Waengler, W. Mier, H. H. Schrenk, M. Bock, L. Schad, and W. Semmler. Synthesis and characterization of HE-24.8: a polymeric contrast agent for magnetic resonance angiography. *Bioconjug. Chem.* **17**:42–51 (2006). doi:10.1021/bc0501909.
34. A. M. Mohs, Y. Zong, J. Guo, D. L. Parker, and Z. R. Lu. PEG-g-poly(GdDTPA-co-L-cystine): effect of PEG chain length on *in vivo* contrast enhancement in MRI. *Biomacromolecules*. **6**:2305–2311 (2005). doi:10.1021/bm050194g.
35. D. R. Messroghli, S. Plein, D. M. Higgins, K. Walters, T. R. Jones, J. P. Ridgway, and M. U. Sivananthan. Human myocardium: single-breath-hold MR T1 mapping with high spatial resolution–reproducibility study. *Radiology*. **238**:1004–1012 (2006). doi:10.1148/radiol.2382041903.
36. J. T. Yap, J. P. Carney, N. C. Hall, and D. W. Townsend. Image-guided cancer therapy using PET/CT. *Cancer J.* **10**:221–233 (2004). doi:10.1097/00130404-200407000-00003.